Micro and Nano Engineering 3 (2019) 37–43

Contents lists available at ScienceDirect

Micro and Nano Engineering

journal homepage: www.journals.elsevier.com/micro-and-nano-engineering

Accelerated publication

Replication of nanoscale surface gratings via injection molding

Olga Muntada-López[a], Jordi Pina-Estany[b], Carles Colominas[b,c], Jordi Fraxedas[d], Francesc Pérez-Murano[a,*], Andres García-Granada[b]

[a] Institute of Microelectronics of Barcelona (IMB-CNM, CSIC), C/Til·lers, Campus Universitat Autònoma de Barcelona. Cerdanyola del Vallès. Barcelona, Spain
[b] GEPI-IQS Grup Enginyeria Producte Industrial, Universitat Ramon Llull, Via Augusta, 390. 08017 Barcelona, (Spain)
[c] Flubetech SL, Carrer Montsià, 23, 08211 Castellar del Vallès, (Spain)
[d] Catalan Institute of Nanoscience and Nanotechnology (ICN2), CSIC, BIST, Campus UAB, Bellaterra, 08193 Barcelona, Spain

ARTICLE INFO

Keywords:
Plastic injection molding
Nanostructured surfaces
Computational fluid dynamics
Heat transfer

ABSTRACT

Nanostructured gratings fabricated on silicon chips have been successfully transferred to polypropylene plastic parts by means of injection molding. Different sets of experiments were carried out along with a repeatability analysis in order to study the effect in the replication of process parameters such as maximum injection pressure, injection time, charge and polymer temperature, geometric factors such as width and separation between lines of the gratings and flow direction as well as demolding conditions. Among all factors, the one with a larger effect is the separation between consecutive trenches, which was studied in detail through Computational Fluid Dynamics simulations. In addition, a previously not reported sinking effect in the nanostructured area and a shrinking of the pattern period were characterized and simulated.

1. Introduction

The development of manufacturing methods for the production of plastic parts with micro/nano scale features is a relevant field of research both in the academic and in the industry realm due to its wide field of applications. These include surface hydrophobicity [1], antireflectivity [2], antimicrobial properties [3], water treatment [4], lab-on-chip devices [5], etc.

Injection molding is a convenient manufacturing process due to its low costs, high replication accuracy and its extended use in industry. However, the replication of nanometer scale features is not a straightforward procedure because the successful replication of the mold largely depends on process and geometrical parameters such as type of polymer [6], mold wall temperature [7,8], structure size [9,10], shear thinning [11], packing conditions [12] and coatings [13] among many others. This is especially relevant for the replication of nanoscale structures with high aspect ratio, since the polymer tends to solidify before it has reached the bottom of the nanocavities.

In the present work, the plastic replication of nanometer scale gratings is studied in detail. The effect of process parameters such as maximum inlet pressure, filling time, charge and polymer temperature in the replication is explored as well as the effect of grating geometry, relative orientation of the grating with regard to the plastic flow and the demolding conditions. Despite the high interest in incorporating nanometer scale features in plastic parts, a precise knowledge of the injection process at nanometer scale is still lacking. This problem is addressed here through the comparison of the experimental results with Finite Volume Method (FVM) simulations that allow the interpretation of the observed phenomenology.

Sinking and shrinking effects were observed by comparing the final dimensions of the plastic parts with the original dimensions of the mold. The result is explained by the combined effect of pressure and temperature at the nanostructured areas.

2. Materials and methods

2.1. Mold manufacturing

Fig. 1(a) and (b) show, respectively, a cross section and a picture of the mold assembly used in the present work and Fig. 1(c) an injected plastic piece with the replica of a grating in the top part. The injected plastic, represented in red colour in Fig. 1(a), flows from right to left in the figure through the ca. 4 mm nozzle advancing radially to meet the nanostructured surface of the silicon chips represented in grey colour. The thickness of the resulting plastic piece is 3 mm while the surface of the silicon chip is at about 1 mm above the mold support. The diameter of the plastic piece is about 50 mm. The mold shown in Fig. 1(b) was made out of stainless steel coated with a DLC film [14]. The

* Corresponding author.
E-mail addresses: francesc.perez@imb-cnm.csic.es (F. Pérez-Murano), andres.garcia@iqs.edu (A. García-Granada).

https://doi.org/10.1016/j.mne.2019.03.003
Received 20 December 2018; Received in revised form 14 March 2019; Accepted 19 March 2019

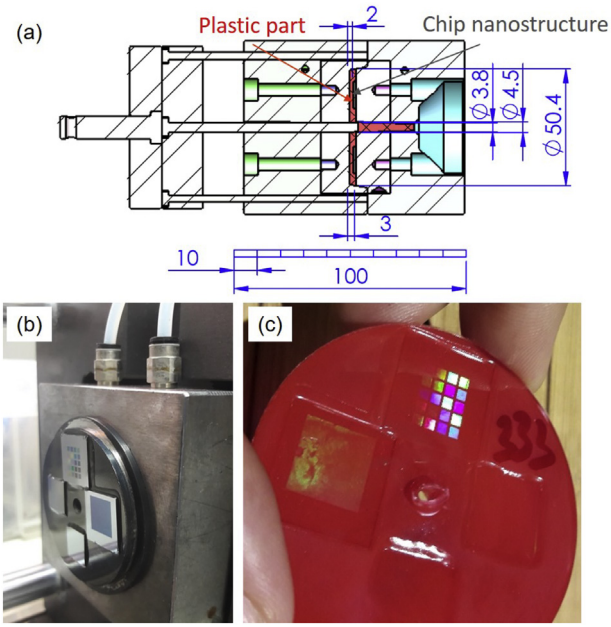

Fig. 1. (a) CAD section of the mold assembly with the critical dimensions (scale in mm). The injected plastic and the silicon mold are represented by red and grey colours, respectively. The plastic injection flows from right to left. (b) DLC-coated stainless steel mold with glued silicon chips. (c) Injected red-colored polypropylene part showing light diffraction in the nanostructured area. (For interpretation of the references to colour in this figure legend, the reader is referred to the web version of this article.)

nanostructured patterns were fabricated in silicon chips, with 15 mm × 15 mm dimensions, and glued with an epoxy adhesive on the injection side of the mold, as can be seen in Fig. 1(b). A red-colored polypropylene (PP) plastic piece replicating the nanometer-size patterns is shown in Fig. 1(c). The replicated area can be easily identified by the colored squares as a consequence of the diffraction of white light induced by the pattern structure that will be introduced below.

2.2. Manufacturing of the nanostructured inserts

The chips were fabricated by standard micro/nano fabrication methods. First, a photolithography process was performed: Fujifilm OiR620-09 photoresist was spun on a standard 4-in. silicon wafer with a final thickness of 0.6 µm, then, selected areas of the wafer were exposed with a NSR-2205-i12D i-line stepper of Nikon with a resolution of 0.35 µm and developed with a OPD-4262 developer (Fujifilm). Second, the resist pattern was transferred into the silicon via reactive ion etching using an Alcatel 601E Deep Reactive Ion Etcher (RIE) with a modified Bosch process to a final depth around 400 nm. Then, the remaining resist on the wafer was removed by over-etching in oxygen plasma (PVA TePla system) and finally, 15 mm × 15 mm chips were cut from the wafer. The nanostructured patterns consisted on arrays of trenches carved in silicon with different dimensions w, s and d_m, as schematized in Fig. 2 (a) and (b), respectively. After injection molding, the cavities in the mold appear as raised features in the plastic part with heights represented by d_{PP}. The chips were glued on the mold in two different configurations, namely with the lines of the gratings both parallel and perpendicular to the direction of the plastic flow, respectively. Fig. 2(c) shows a picture of a silicon chip where the gratings can be easily identified as colored squares as well as SEM images of one grating with details of the patterns at different scales.

2.3. AFM and SEM characterization

The manufactured silicon patterns were characterized prior to the plastic injection using a Zeiss Auriga scanning electron microscope to determine the s and w parameters, as shown in Fig. 1(c). The accurate dimensions of the trenches were determined by means of a Bruker ICON atomic force microscope (AFM) operated in tapping mode using OTESPA cantilevers.

Four combinations of geometric parameters of the trench arrays were selected, with nominal values s = 500 and 1000 nm and w = 500 and 1000 nm, respectively, in order to analyze the dependence of the replication on the dimensions of the trenches (see Table 1). These values were used in the simulations for the sake of clarity. It can be observed that the measured values are quite close to the nominal one. The trench depth d_m shows some dispersion from the target 400 nm value; for trenches b and d (s = 500 nm), it is lower than for trenches a and c (s = 1000 nm), differences that can be attributed to the etching process.

2.4. Injection molding

The injections were performed in a Babyplast 6/10P, a micro injection molding machine, with raw material SABIC© PP 621P, a PP random copolymer for cast film with a melt flow rate of 8.0 dg/min at 230 °C and 2.16 kg according to ISO 1133 standards and to the manufacturer. Previous experiments using polycarbonate (PC) were used as starting conditions to design a set of experiments in order to analyze the influence of first and second injection pressures (P_i and P_h, respectively), injection (t_i) and holding times (t_h), polymer temperature (T_P) and new parameters such as the stroke of pressure piston or charge (C) [14]. The injection pressure is applied from zero to P_i during t_i seconds, with a fraction of this time at constant P_i. After t_i the pressure is reduced to P_h and applied during t_h seconds.

With the aim of stabilizing and ensuring the optimal machine performance, tens of test injections were done before every injection set. After that, a first injection was performed with the selected conditions in order to confirm the viability of the process (complete mold filling, easy detachment from the mold, no polymer burning, etc.) and then, a minimum of two additional parts were injected. In order to avoid possible interferences with the previous parameters the first injected part was always discarded. The injections were done on the same day in order to minimize the influence of external factors. Additionally, a specific analysis was carried out to confirm repeatability (see Supplemental Information I). Thermal imaging was used during the injection to monitor the temperature of the polymer and mold walls (See Supplemental Information II). The velocity of the polymer melt ranged from 60 mm/s near the inlet to 40 mm/s at the end of nanostructured zone where the thickness of the plastic part is reduced from 3.0 down to 2.5 mm. After > 500 injections no significant changes were observed on the silicon patterned area of the mold. This validates the stability of silicon inserts in small batches used for the prototyping of plastic parts.

3. Results and discussion

3.1. Influence of mold geometric parameters on the replication fidelity

We analyze first the influence of the w and s parameters on the efficiency of the replication process when the direction of the plastic flow is perpendicular to the direction of the lines of the gratings [see Fig. 2(c)]. We define the fidelity factor (f) as the ratio between d_{PP} and d_m; $f = d_{PP}/d_m$ [see Fig. 2(b)]. The different injection conditions used, A to E, are described in Fig. 3 and the replication depth d_{PP} of the trenches is determined by AFM for four combinations of w and s, 0.5 and 1 µm.

From Fig. 3 it becomes obvious that the geometrical factor with a major effect on the height of the replicated plastic nanostructures is the distance between consecutive trenches (w); the smaller this parameter is, the deeper the polymer penetrates into the cavities achieving a maximum fidelity factor f = 0.7. To our knowledge, this observation is

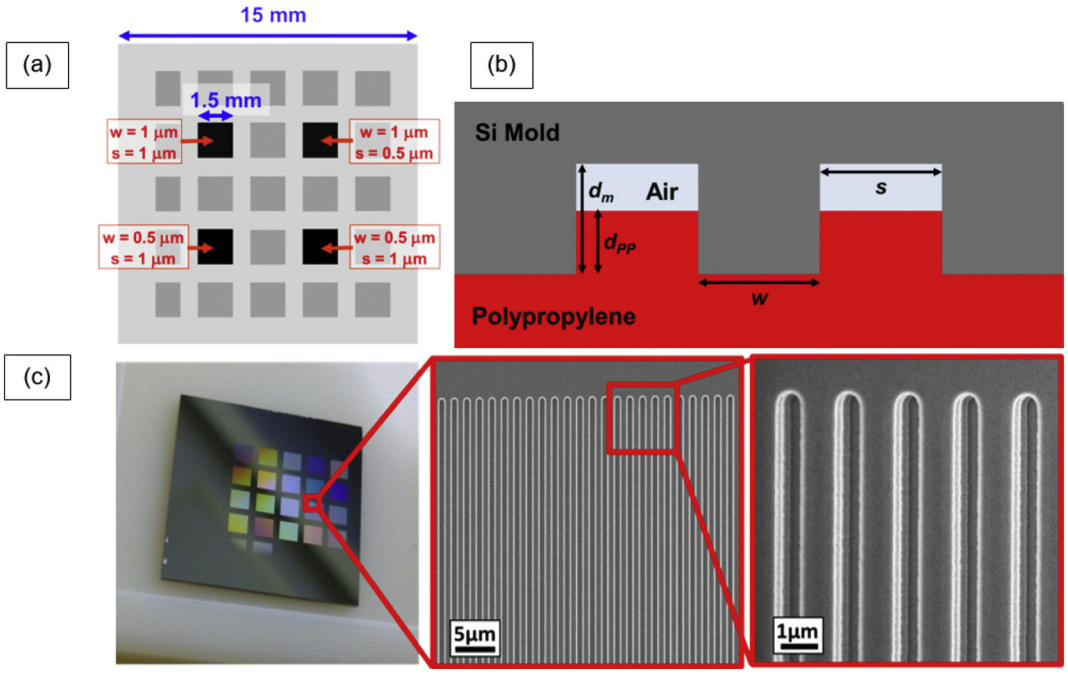

Fig. 2. (a) Scheme of a silicon chip showing the relevant dimensions. (b) Cartoon of the cross section of the micro/nanostructures on the silicon (grey) and polypropylene (red) parts defining the dimensional parameters: w and s (horizontal) and d_m and d_{PP} (vertical). (c) Picture of a silicon chip with the patterns grating revealed by diffraction of white light and SEM images of one grating showing details of the patterns at different scales. (For interpretation of the references to colour in this figure legend, the reader is referred to the web version of this article.)

Table 1
Silicon chip nominal and measured values for s, w and d_m parameters.

Trench array	w nom. (nm)	s nom. (nm)	w real (nm)	s real (nm)	d_m AFM (nm)	d_m SEM (nm)
a	1000	1000	995	1020	413	428
b	1000	500	995	525	363	377
c	500	1000	500	1020	417	432
d	500	500	470	540	367	381

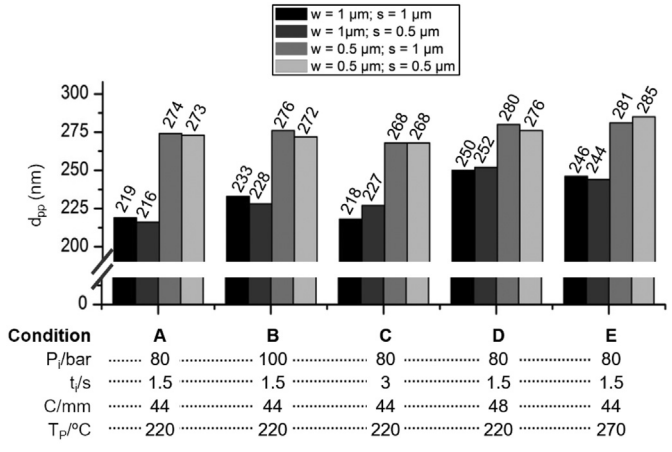

Fig. 3. Set of experiments for quantifying the effect of four factors in the nanocavities replication (maximum inlet pressure, injection time, charge and polymer melt temperature). Legend depicts nominal values, real values are found in Table 1.

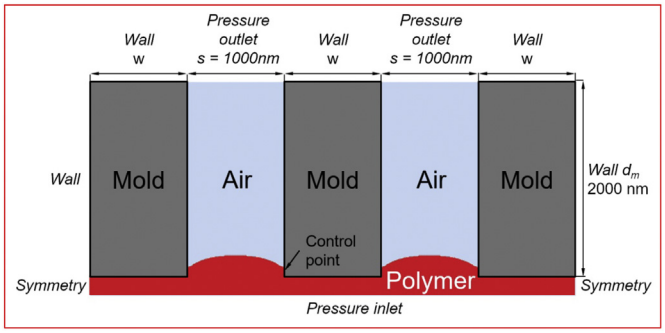

Fig. 4. Model used for analyzing the impact of w in the replication of nanocavities. The control point is located 40 nm above the mold surface.

not previously reported in the literature and it deserves a detailed analysis. This effect can be explained by the fact that a smaller w value leads to a warming of the mold walls between consecutive cavities and, hence, the replicated depth increases as if the polymer was effectively injected at a higher mold temperature. Mold temperature has been reported as a factor with a large positive effect in the replication depth by many authors including for simulations and injections of microcantilever structures [15], for microcantilevers with different aspect ratio [16] and for nanocavities with a submodeling simulation approach [14], among others. In order to prove this hypothesis, a 2D CAD model was created with adjustable w dimension and a temperature control point was set at the mold surface, as depicted in Fig. 4. In order to analyze the mold temperature increase the model takes into consideration two consecutive trenches.

The submodeling approach described in [14,17] was used in the simulations. This algorithm overcomes the computational impossibility of carrying a simulation of a macroscopic part with a nanoscale mesh. First, a global simulation of injection molding was performed with the Solidworks Plastics software without considering nanometer features and, second, the results of this simulation were used as boundary conditions in a second nanoscale computational fluid dynamics

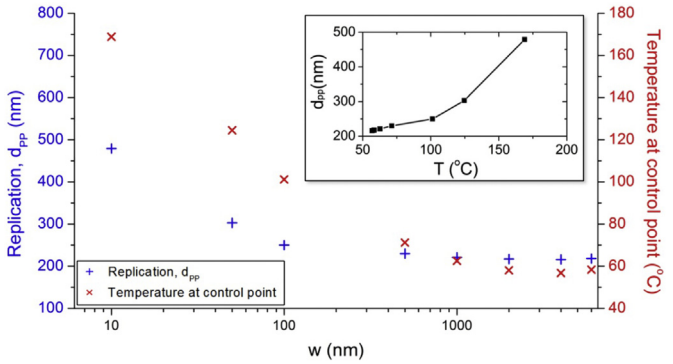

Fig. 5. Simulated results of the impact of w for s = 1 μm in the replication of nanocavities. For w < 1 μm a clear tendency can be observed: smaller w leads to higher temperatures at the control point (red) and higher replications (blue). On the other hand, this tendency was not observed for w > 1 μm. Inset: Simulation of the depth reached by the polymer depending on the temperature. (For interpretation of the references to colour in this figure legend, the reader is referred to the web version of this article.)

simulation performed using the ANSYS Fluent software. The simulations used the following parameters: P_i = 80 bar, t_i = 1.5 s, C = 44 mm, T_P = 220 °C and mold temperature of 50 °C, and w was varied from 0.01 μm up to 6 μm in order to study its effect on the replication and in the control point temperature. The results are shown in Fig. 5.

The simulation results are consistent with the hypothesis of larger replication due to the warming of the mold wall between nanotrenches. Simulations showed a negligible influence of the s parameter in the replication. Indeed, the simulation shows an increase of the control point temperature with smaller w dimensions (right axis of Fig. 5) and this leads to a larger replication of the nanocavity (left axis of Fig. 5). It is also observed that there is a threshold w dimension, around 1 μm, above which the effect of w becomes negligible. Fig. 6 depicts the simulated temperature profile once the polymer reaches the no flow temperature (NFT) for w = 1 μm [Fig. 6(a)] and w = 0.1 μm [Fig. 6(b)] confirming that the mold between nanotrenches reaches larger temperatures for smaller w dimensions. The NFT was set to 60 °C in the simulation.

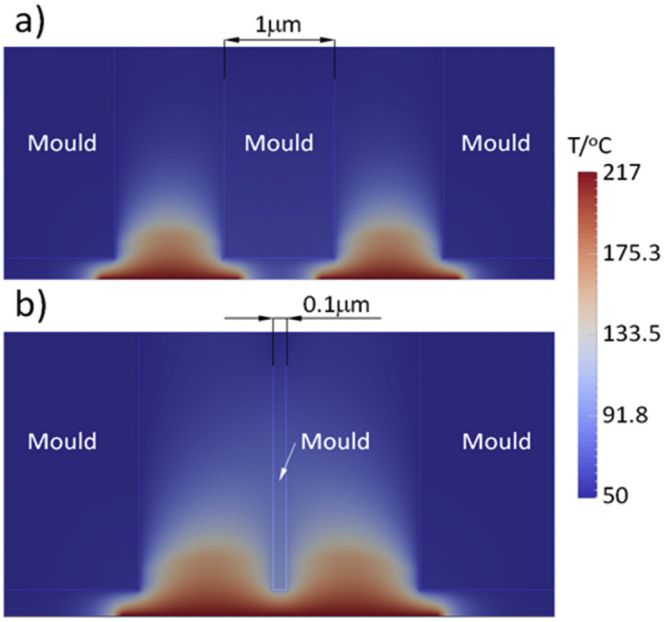

Fig. 6. Temperature distribution once the polymer reaches the no flow temperature for wall width w = 1 μm (top) and w = 0.1 μm (bottom). Trench width is s = 1 μm in both cases.

In order to investigate the precision of the tests, a repeatability analysis was performed. A total of 12 parts, 6 at 220 °C and 6 more at 270 °C were injected for the equivalent four combinations of w and s. The average standard deviation (1σ) of the height measurements was of 4.4 nm confirming that the replication process is repeatable and that the observed behavior is significant (See Supplemental Information I).

Additional experiments were carried out to prove that the demolding time did not affect the replication of the cavities either when the two sides of the mold were separated or in contact. The results can be found in the Supplemental Information III.

3.2. Analysis of the replication fidelity

Fig. 7 shows cross sections of AFM images of the mold (black continuous lines) and of the PP part (red continuous lines). The direction of the plastic flow is indicated in the figure, which is perpendicular [Fig. 7(a)] and parallel [Fig. 7(b)] to the direction of the lines of the gratings, respectively. The injections for both directions were performed in separate experiments using different silicon molds. The nominal w and s parameters are w = 0.5 μm and s = 1 μm in Fig. 7(a) and w = 0.75 μm and s = 0.5 μm in Fig. 7(b), respectively. In both cases P_i and t_i were set to 80 bar and 1.5 s, respectively, and the polymer temperature to 200 and 220 °C in Fig. 7(a) and (b), respectively, and the polymer charge 48 and 19 mm in Fig. 7(a) and (b), respectively.

In each figure the left and right part correspond to the plastic flow entering and exiting the mold pattern, respectively. The scale of the mold curve has been inverted in order to facilitate the comparison. Two salient effects are observed: (i) the PP never reaches the bottom of the trenches and the base line of the replicated region lies below the base line corresponding to the plastic region in contact with the flat silicon surface, which is represented by Δh (sinking effect) and (ii) the period of the replicated pattern is smaller than that corresponding to the mold (shrinking effect). Both effects are studied next.

3.2.1. Sinking effect

As mentioned above the replicated grating appears below the ground level of the region without grating. Fig. 8 shows the measured heights due to sinking both at the entry (Δh_{entry}) and exit (Δh_{exit}) in the case of the polymer flow perpendicular to the direction of the trenches for the experimental conditions depicted in Table 1 and Fig. 3. From the figure it can be concluded that no clear difference between Δh_{entry} and Δh_{exit} is observed but that the values are clearly higher for smaller trench separations (w). In this case the polymer is at higher temperature, as discussed in Section 3.1, and as a consequence the polymer fills more fraction of the cavity as compared to the case of larger w and, therefore the pressure increases more. In addition, at higher temperatures the Young's modulus of the polymers decreases becoming more easily deformed (see Discussion below).

An analogous analysis for the case of the plastic flowing parallel to the trenches leads to similar results, as evidenced in Fig. 7(b). For such analysis a mold with w = 0.7 μm (nominal 0.75 μm) and s = 0.55 μm (nominal 0.5 μm) was used with the following injection parameters: P_i = 80 bar, t_i = 1.5 s, C = 19 mm and T_P = 220 °C. In this case we obtained a sinking depth of 60 nm and a penetration d_{pp} of 190 nm.

We attribute the sinking of the replicated pattern to the trapping of air in the cavities of the mold. The polymer completely covers the full cavity of the mold in < 0.6 s, since the velocity of the polymer melt at the end of the mold is about 40 mm/s and the radius of the mold is 25 mm [see Fig. 1(a)]. Moreover, the polymer melt flows over the silicon mold in < 0.4 s, since the lateral dimensions are 15 mm × 15 mm and for an individual pattern (1.5 mm × 1.5 mm) this time is < 0.04 s. However, the injection time is above 1 s, so that the patterns of the mold are already covered when the polymer is still in the phase of filling the cavities. The advance of the melted polymer in the cavities compresses the trapped air, thus increasing its pressure following the

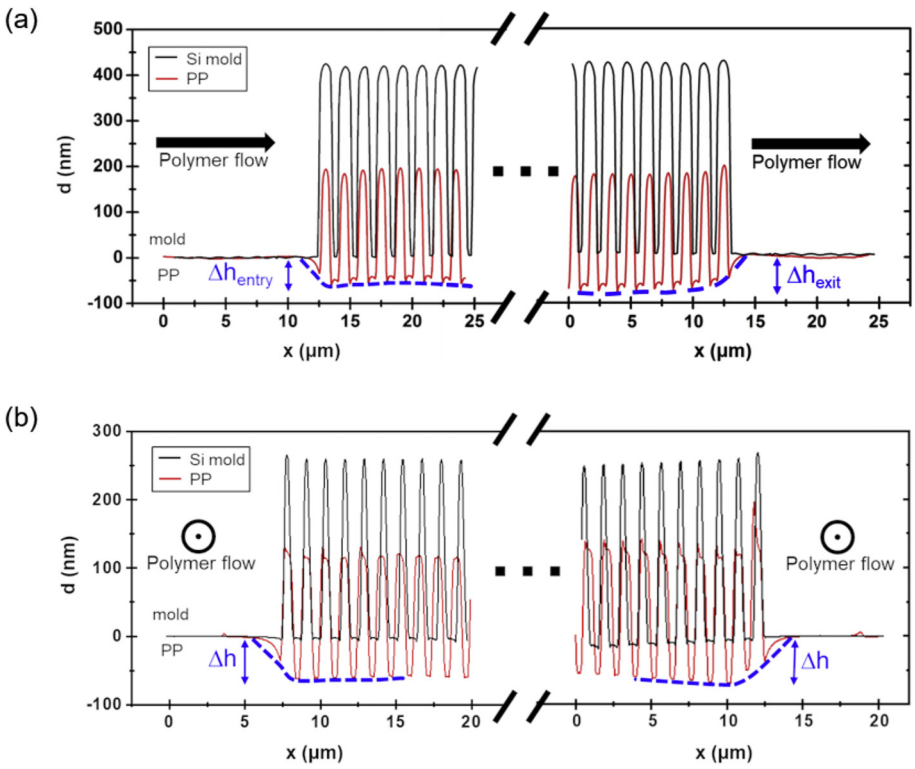

Fig. 7. Superposed AFM cross sections of the polymer (continuous red line) and mold (continuous black line) at the flow entry (left) and exit (right) of the pattern. (a) w = 0.5 μm and s = 1 μm (nominal), P_i = 80 bar, t_i = 1.5 s, T_P = 200 °C and C = 48 mm. (b) w = 0.75 μm and s = 0.5 μm (nominal), P_i = 80 bar, t_i = 1.5 s, T_P = 220 °C and C = 19 mm. (For interpretation of the references to colour in this figure legend, the reader is referred to the web version of this article.)

Boyle's law [18] and, therefore, hindering the polymer progress. Therefore, the sinking should appear regardless of the orientation, as has been experimentally demonstrated.

Fig. 9 shows the prediction of the sinking effect arising from simulations for w and s values of 0.5 and 1 μm and at two different pressures of 0.2 and 0.4 MPa corresponding to trapped air in the cavities. The simulations considered a 2D layer of 1 μm thickness. The polymer Young's modulus was reduced from 800 MPa at room temperature down to 20 MPa for the simulation of air trapped at high temperature following previously reported results [19]. Air is initially set to atmospheric pressure of approximately 0.1 MPa. When air is compressed to one fourth of its original volume the pressure increases up to 0.4 MPa. When the replication height is only reduced to half of the trench height the pressure is only 0.2 MPa. Then, the resultant force applied to plastic is the summation of number of marks multiplied by the surface area of each mark. Note that the colour scale in the figure reflects displacements referred to unperturbed regions sufficiently away from mold.

From the simulations we can conclude that the sinking effect depends on the trench density, obtaining a displacement Δh of 81.8 nm for w = 0.5 and s = 1 μm. However, a very small influence of w on Δh is observed, as evidenced when comparing Fig. 9 (b) and (c). The reason is that the reduction of the Young's modulus with temperature has to be considered. If the Young's modulus decreases, the polymer penetrates more into the trenches, increasing the effective pressure (less volume and more temperature of trapped air), and so, enhancing the sinking effect. The sinking is very sensitive to pressure, as it is shown by comparing Fig. 9(a) and (b) with Fig. 9(e) and (f), when the pressure of

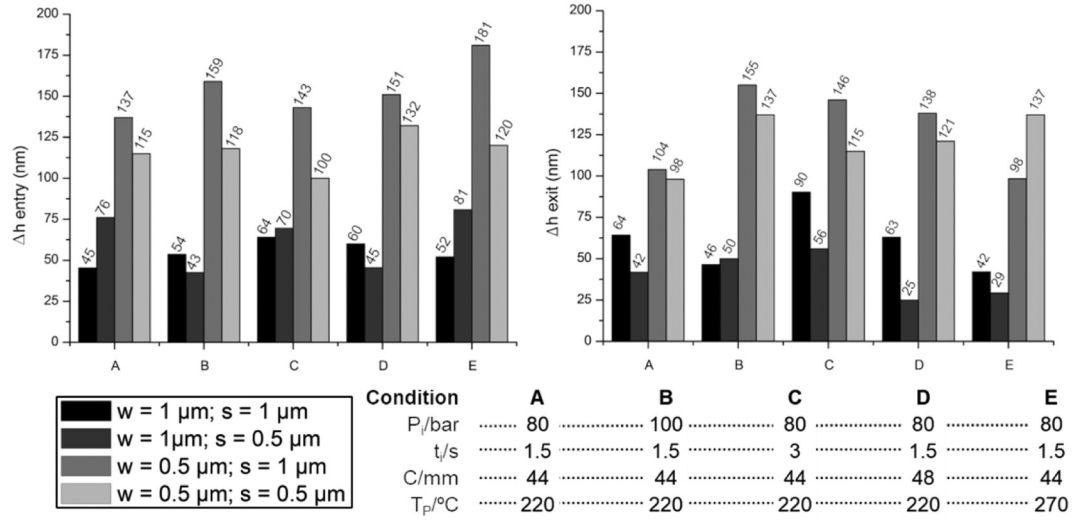

Fig. 8. Study of the sinking effect at the entry (left) and at the exit (right) of the silicon chip for different process conditions and plastic flow perpendicular to the lines of the gratings. The legend depicts nominal values. The actual values are found in Table 1.

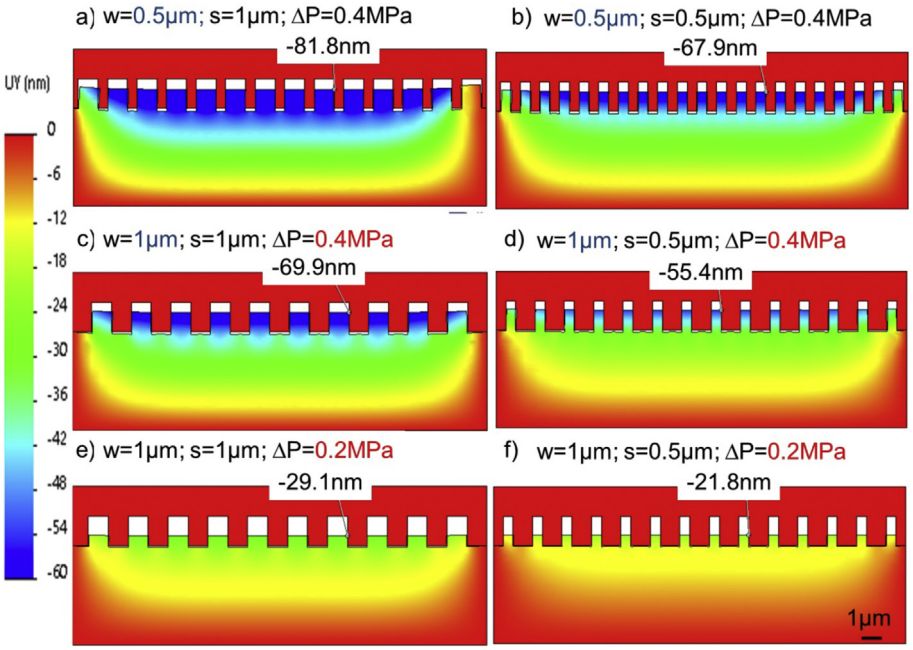

Fig. 9. Simulated displacements of a replicated mold using a colour code using the following parameters: (a) w = 0.5 μm, s = 1 μm, 0.4 MPa, (b) w = 0.5 μm, s = 0.5 μm, 0.4 MPa, (c) w = 1 μm, s = 1 μm, 0.4 MPa, (d) w = 1 μm, s = 0.5 μm, 0.4 MPa, (e) w = 1 μm, s = 1 μm, 0.2 MPa and (f) w = 1 μm, s = 0.5 μm, 0.2 MPa.

trapped air is reduced from 0.4 MPa to 0.2 MPa. Note that at higher pressures the polymer separates from the mold in the regions defined by the w parameter [see Fig. 2(b)]. Thus, simulations of sinking effect are useful if the larger temperatures achieved on thinner walls, where a major replication is observed, are taken into account.

3.2.2. *Shrinking effect*

As pointed out when describing Fig. 7, the period of the replicated grating is smaller than that corresponding to the silicon mold and we attribute this result to the thermal contraction of the plastic part once separated from the mold. In order to explore the effect of thermal contraction we have performed a conventional plastic injection simulation to estimate the size of the volumetric shrinking in the whole plastic part [see Fig. 10(a)]. From the figure we observe that the predicted volumetric shrinking varies from about 10% in the area close to the center of the plastic disc to about 5% in the radial direction. An additional simulation of the effect of thermal expansion considering the gratings was carried out and the results are shown in Fig. 10(b). The initial temperature was set to 220 °C for the polymer and 50 °C for the mold. The thermal expansion coefficient for polypropylene was set to $1.6 \cdot 10^{-4}\,K^{-1}$ and to $1.6 \cdot 10^{-5}\,K^{-1}$ for the silicon chip, which is an order of magnitude smaller (the thermal expansion of steel, $2 \cdot 10^{-5}\,K^{-1}$, is similar to that of silicon). Fig. 10(b) shows a clear decrease of the polymer period, with a total shrinking of 420 nm, after cooling down to 20 °C after separation of the plastic part and mold and overlapping with the mold as it is shown experimentally in Fig. 7.

4. Conclusions

Plastic injection is an inexpensive, fast and established technique suitable for replicating micro/nanostructures at industrial level. Silicon chips glued onto conventional injection molds provide a fast and simple method for experimental investigation of the injection process applied to the replication of nanostructures. The replication of nanoscale gratings has been investigated and different phenomena have been identified that will be relevant for the future development of plastic injection as a method for high volume fabrication of nanostructured surfaces.

From the experimental analysis of dimensional parameters, it is concluded that the width of the trenches in the mold is a factor of minor significance in the investigated dimensions range (between 0.5 and

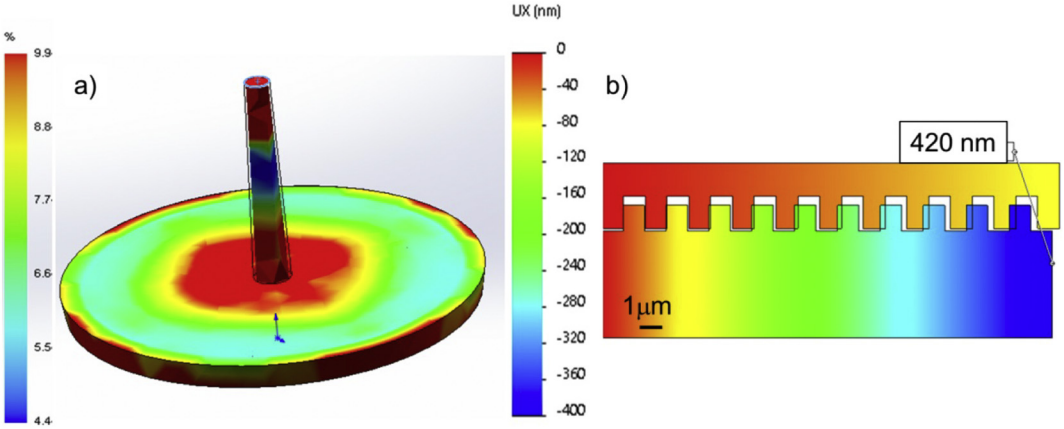

Fig. 10. (a) Volume shrinking simulation with conventional plastic injection simulation and (b) thermal contraction of steel mold with silicon chip on top compared to plastic part bottom to justify different period in trenches at 20 °C after cool down.

1 μm). However, the trench separation plays a key role in the dimensions of the features in the plastic part: thinner walls lead to a more efficient heat transfer and thus to a more accurate polymer replication. The trench separation effect was found to be significant for w values below 1 μm, as corroborated by Computational Fluid Dynamics simulations.

Remarkably, a sinking in the nanostructured area of the polymer part is found out, ranging from 25 to 180 nm depending on the injection molding conditions. This sinking effect is attributed to the combined effect of the pressure effectuated by the trapped air in the pattern area and to the local lowering of polymer Young's modulus in this region.

In addition, a shrinking of the pattern period is observed which is due to the thermal contraction of the plastic part once it is removed from the mold. Simulations predict a shrinking ranging from about 4.4% to 10%.

Finally, no difference in the replication accuracy was observed for different demolding conditions, including different cooling times and temperatures.

Acknowledgements

This work has been performed within the aim4np project (Automated in-line Metrology for Nanoscale Production), supported by the EC [grant number 309558] within the 7th Frame-work Program NMP on Nanoscale mechanical metrology for industrial processes and products. The ICN2 is funded by the CERCA Program/Generalitat de Catalunya. The ICN2 is supported by the Severo Ochoa program of the Spanish Ministry of Economy, Industry and Competitiveness MINECO [grant number SEV-2017-0706].

Appendix A. Supplementary data

Supplementary data to this article can be found online at https://doi.org/10.1016/j.mne.2019.03.003.

References

[1] Y.E. Yoo, T.H. Kim, D.S. Choi, S.M. Hyun, H.J. Lee, K.H. Lee, S.K. Kim, B.H. Kim, Y.H. Seo, H.G. Lee, J.S. Lee, Injection molding of a nanostructured plate and measurement of its surface properties, Curr. Appl. Phys. 9 (2009) e12–e18, https://doi.org/10.1016/j.cap.2008.12.023.

[2] A.B. Christiansen, J.S. Clausen, N.A. Mortensen, A. Kristensen, Injection moulding antireflective nanostructures, Microelectron. Eng. 121 (2014) 47–50, https://doi.org/10.1016/j.mee.2014.03.027.

[3] S. Kim, U.T. Jung, S.K. Kim, J.H. Lee, H.S. Choi, C.S. Kim, M.Y. Jeong, Nanostructured multifunctional surface with antireflective and antimicrobial characteristics, ACS Appl. Mater. Interfaces 7 (2015) 326–331, https://doi.org/10.1021/am506254r.

[4] S. Baruah, S. K. Pal, J. Dutta, Nanostructured zinc oxide for water treatment, Nanosci. Technol. 2 (2012) 90–102, https://doi.org/10.2174/2210681211202020090.

[5] H.J. Oh, J.H. Park, S.J. Lee, B. Il Kim, Y.S. Song, J.R. Youn, Sustainable fabrication of micro-structured lab-on-a-chip, Lab Chip 11 (2011) 3999–4005, https://doi.org/10.1039/c1lc20441f.

[6] K. Monkkonen, T.T. Pakkanen, J. Hietala, E.J. Pakkonen, P. Pakkonen, T. Jskelinen, T. Kaikuranta, Replication of sub-micron features using amorphous thermoplastics, Polym. Eng. Sci. 42 (2002) 1600–1608, https://doi.org/10.1002/pen.11055.

[7] S. Kuhn, A. Burr, M. Kübler, M. Deckert, C. Bleesen, Study on the replication quality of micro-structures in the injection molding process with dynamical tool tempering systems, Microsyst. Technol. 16 (2010) 1787–1801, https://doi.org/10.1007/s00542-010-1104-y.

[8] S. Hattori, K. Nagato, T. Hamaguchi, M. Nakao, Rapid injection molding of high-aspect-ratio nanostructures, Microelectron. Eng. 87 (2010) 1546–1549, https://doi.org/10.1016/j.mee.2009.11.028.

[9] C. Rytka, P.M. Kristiansen, A. Neyer, Iso- and Variothermal Injection Compression Moulding of Polymer Micro- and Nanostructures for Optical and Medical Applications, 25 (2015), https://doi.org/10.1088/0960-1317/25/6/065008.

[10] H. Schift, C. David, M. Gabriel, J. Gobrecht, L.J. Heyderman, W. Kaiser, S. Köppel, L. Scandella, Nanoreplication in polymers using hot embossing and injection molding, Microelectron. Eng. 53 (2000) 171–174, https://doi.org/10.1016/S0167-9317(00)00289-6.

[11] T.R. Tofteberg, Injection Molding of Microfeatured Polymer Components, Doctoral Dissertation by (2009), p. 118.

[12] M. Zhou, B. Jiang, C. Weng, L. Zhang, Experimental study on the replication quality of micro–nano cross-shaped structure arrays in injection molding, Microsyst. Technol. 23 (2017) 983–989.

[13] M. Matschuk, H. Bruus, N.B. Larsen, Nanostructures for all-polymer microfluidic systems, Microelectron. Eng. 87 (2010) 1379–1382, https://doi.org/10.1016/j.mee.2009.11.167.

[14] J. Pina Estany, C. Colominas, J. Fraxedas, J. Llobet, F. Perez Murano, J.M. Puigoriol Forcada, D. Ruso, A.A. García Granada, A statistical analysis of nanocavities replication applied to injection moulding, Int. Commun. Heat Mass Transf. 81 (2017) 131–140.

[15] B. Sha, S. Dimov, C. Griffiths, M.S. Packianather, Micro-injection moulding: factors affecting the achievable aspect ratios, Int. J. Adv. Manuf. Technol. 33 (2007) 147–156, https://doi.org/10.1007/s00170-006-0579-2.

[16] W.W. Kim, M.G. Gang, B.K. Min, W.B. Kim, Experimental and numerical investigations of cavity filling process in injection moulding for microcantilever structures, Int. J. Adv. Manuf. Technol. (2014) 293–304, https://doi.org/10.1007/s00170-014-6104-0.

[17] T. Tofteberg, E. Andreassen, Injection moulding of microfeatured components, Proc. Polym. Process. Soc. 24th Annu. Meet. PPS-24, 2008 http://www.sintef-norge.com/project/mpc/Tofteberg2-PPS-2008.pdf.

[18] P.a. Tipler, G. Mosca, Physics for Scientists and Engineers, (2009) (doi:013613923X).

[19] C. Stern, On the Performance of Polypropylene: Between Synthesis and End-Use Properties, University of Twente, 2005.